Molecular Pharmacology Fast Forward. Published on July 23, 2014 as DOI: 10.1124/mol.114.094128
This article has not been copyedited and formatted. The final version may differ from this version.

A role for picomolar concentrations of pregnenolone sulfate in synaptic activity-dependent Ca^{2+} signaling and CREB activation

Conor C. Smith, Stella C. Martin, Kavitha Sugunan, Shelley J. Russek, Terrell T. Gibbs, David H. Farb

Laboratory of Molecular Neurobiology (CCS, SCM,KS, TTG, DHF), Department of Pharmacology & Experimental Therapeutics, Laboratory of Translational Epilepsy (SJR), Boston University School of Medicine, 72 East Concord Street, Boston, Massachusetts 02118, USA.

Downloaded from molpharm.aspetjournals.org at ASPET Journals on March 20, 2024

Molecular Pharmacology Fast Forward. Published on July 23, 2014 as DOI: 10.1124/mol.114.094128
This article has not been copyedited and formatted. The final version may differ from this version.

Running title: Picomolar pregnenolone sulfate activates synaptic activity & CREB

Corresponding author:
David H. Farb
Boston University School of Medicine, 72 East Concord Street, Boston, Massachusetts 02118, USA
E-mail: dfarb@bu.edu
Tel: 617-638-4481
Fax: 617-638-4329

Text pages excluding Abstract and References and legends: 16
Tables: 0
Figures: 7
References: 59
Abstract: 245 words
Introduction: 580 words
Discussion: 993 words

Non-standard Abbreviations:
1-[2-(3,4-Dichlorophenyl)ethyl]-4-methylpiperazine dihydrochloride, **BD 1063**; cAMP response element-binding protein, **CREB**; dimethyl sulfoxide, **DMSO**; half maximal effective concentration, **EC_{50}**; extracellular-signal-regulated kinase/mitogen-activated protein kinase, **ERK/MAPK**; N-[2-[[[3-(4-Chlorophenyl)-2-propenyl]methylamino]methyl]phenyl]-N-(2-hydroxyethyl)-4-methoxybenzenesulphonamide, **KN-93**; long term potentiation, **LTP**; (5S,10R)-(+)-5-Methyl-10,11-dihydro-5H-dibenzo[a,d]cyclohepten-5,10-imine hydrogen maleate, **MK-801**; N-methyl D-aspartate receptor, **NMDAR**; pregnenolone sulfate, **PregS**; (α R, β S)-α -(4-Hydroxyphenyl)- β -methyl-4-(phenylmethyl)-1-piperidinepropanol maleate, **Ro 25-6981**; standard error of the mean, **SEM**; store operated calcium channel, **SOCC**; 1,4-Diamino-2,3-dicyano-1,4-bis[2-aminophenylthio]butadiene, **U0126**; vehicle, **VEH**

Downloaded from molpharm.aspetjournals.org at ASPET Journals on March 20, 2024

Molecular Pharmacology Fast Forward. Published on July 23, 2014 as DOI: 10.1124/mol.114.094128
This article has not been copyedited and formatted. The final version may differ from this version.

Abstract

Fast excitatory synaptic transmission that is contingent upon N-methyl D-aspartate receptor (NMDAR) function contributes to core information flow in the central nervous system (CNS) and to the plasticity of neural circuits that underlie cognition. Hypoactivity of excitatory NMDAR-mediated neurotransmission is hypothesized to underlie the pathophysiology of schizophrenia, including the associated cognitive deficits. The neurosteroid pregnenolone (PREG) and its metabolites pregnenolone sulfate (PregS) and allopregnanolone in serum are inversely associated with cognitive improvements following oral PREG therapy, raising the possibility that brain neurosteroid levels may be modulated therapeutically. PregS is derived from PREG, the precursor of all neurosteroids, via a single sulfation step and is present at low nanomolar concentrations in the CNS. PregS, but not PREG, augments LTP and cognitive performance in animal models of learning and memory. In this report, we communicate the first observation that PregS, but not PREG, is a potent (EC_{50} ~ 2 pM) enhancer of intracellular Ca^{2+} that is contingent upon neuronal activity, NMDAR-mediated synaptic activity, and L-type Ca^{2+} channel activity. Low pM PregS similarly activates CREB phosphorylation (within 10 min), an essential memory molecule, via an ERK/MAPK signal transduction pathway. Taken together, the results are consistent with a novel biological role for the neurosteroid PregS that acts at picomolar concentrations to intensify the intracellular response to glutamatergic signaling at synaptic, but not extra-synaptic, NMDARs by differentially augmenting CREB activation. This provides a genomic signal transduction mechanism by which PregS could participate in memory consolidation of relevance to cognitive function.

Downloaded from molpharm.aspetjournals.org at ASPET Journals on March 20, 2024

Molecular Pharmacology Fast Forward. Published on July 23, 2014 as DOI: 10.1124/mol.114.094128
This article has not been copyedited and formatted. The final version may differ from this version.

Introduction

The neurosteroid pregnenolone sulfate (PregS) has been known to act as a cognitive enhancer and modulator of neurotransmission for 20 years, yet aligning its pharmacological and physiological effects with reliable measurements of endogenous local concentrations has remained elusive (reviewed in Gibbs *et al*., 2006; Schumacher *et al*., 2008). Recent findings highlight the potential for neurosteroid treatment of neurological and neuropsychiatric disorders (Bibb *et al.*, 2010; Collingridge *et al.*, 2013) via the action of a pregnenolone (PREG) metabolite(s) including PregS (Marx *et al.*, 2009). PREG is synthesized *de novo* in the brain from cholesterol and is enriched in nervous tissue compared to its levels in cerebrospinal fluid, serum and/or plasma in both humans and rodents (Weill-Engerer *et al.*, 2002; Marx *et al.*, 2006, 2009; Naylor *et al.*, 2008; Caruso *et al.*, 2013). PREG or one of its metabolites has also emerged as a negative feedback modulator of cannabinoid receptor subtype-1 signaling (Vallée *et al.*, 2014), raising the possibility that neurosteroids could be viable therapeutics for the treatment of cannabis intoxication.

PREG improves cognitive deficits associated with schizophrenia in a way that correlates inversely with the lowest concentrations of its downstream neurosteroid metabolites in serum, including PregS, PREG, and allopregnanolone (Marx *et al.*, 2009; Ritsner *et al.*, 2010, 2014; Kreinin *et al.*, 2014). PregS enhances the performance of rodents in models of cognition (Mayo *et al.*, 1993; Flood *et al.*, 1995; Vallée *et al.*, 1997; Akwa *et al.*, 2001; Darnaudéry *et al.*, 2002), and NMDAR contingent spatial memory (Petit *et al.*, 2011; Plescia *et al.*, 2013). PregS is present in rodent (Rustichelli *et al.*, 2013) and human brain (Weill-Engerer *et al.*, 2002; Liere *et al.*, 2004) at physiologically

Downloaded from molpharm.aspetjournals.org at ASPET Journals on March 20, 2024

Molecular Pharmacology Fast Forward. Published on July 23, 2014 as DOI: 10.1124/mol.114.094128
This article has not been copyedited and formatted. The final version may differ from this version.

relevant concentrations. PregS enhances excitatory synaptic transmission by both presynaptic and postsynaptic mechanisms with potencies in the micromolar range (Wu *et al.*, 1991; Park-Chung *et al.*, 1997; Wagner *et al.*, 2008). PregS, but not PREG, potentiates NMDAR responses (Wu *et al*., 1991, Malayev *et al*. 2002), enhances NMDAR trafficking to the cell surface (Kostakis *et al.*, 2013) via a Ca^{2+} dependent G-protein coupled mechanism, and enhances LTP (Sliwinski *et al.*, 2004; Chen *et al.*, 2007) in an NMDAR dependent fashion. It is also known that PregS can be released in a retrograde messenger-like fashion to increase presynaptic glutamate release (Mameli *et al.*, 2005).

We sought to determine whether physiologically relevant concentrations of PregS could initiate a sequence of molecular events that potentially lead to cognitive enhancement. The results demonstrate that, contingent upon synaptic NMDAR activation, PregS, but not PREG, increases the concentration of intracellular Ca^{2+} ($[Ca^{2+}]_i$) with a potency of 2 pM in an NMDAR- and L-type Ca^{2+} channel (Ca^{2+}_L) contingent manner. Moreover, neuronal activity, Ca^{2+}_L, and functional synaptic but not extrasynaptic NMDAR activity are required for low pM PregS-activated CREB phosphorylation.

The results provide further support for PregS as a high affinity positive modulator of synaptic function consistent with its actions as a cognitive enhancer. While the endogenous role of PregS in modulating synaptic activity remains an area of open investigation, the results reported here demonstrate that low pM concentrations of PregS induce increases in Ca^{2+} and pCREB in a manner that requires excitatory synaptic (but not extrasynaptic) transmission and is contingent upon NMDAR, likely NR2B subtype

Downloaded from molpharm.aspetjournals.org at ASPET Journals on March 20, 2024

Molecular Pharmacology Fast Forward. Published on July 23, 2014 as DOI: 10.1124/mol.114.094128
This article has not been copyedited and formatted. The final version may differ from this version.

selective, activation. PregS might act to reduce cognitive dysfunction in schizophrenia by reducing NMDAR hypofunction (Javitt, 2007; Millan, 2005; Coyle, 2006; Rujescu *et al.*, 2006) and activating CREB phosphorylation, a transcription factor critical in the maintenance of LTP (Bourtchuladze *et al.*, 1994; Ahmed and Frey, 2005).

Materials and Methods

***Neuronal cell culture*:** Embryonic (E18, mixed sex) rat cortical cells or hippocampal cells were isolated and cultured as in (Russek *et al.*, 2000) for 6-8 days (cortical) or 21-28 days (hippocampal) *ex vivo* and used in confocal imaging or western blots For analysis of pCREB and pERK, cells were plated on poly-L-lysinated (0.1 mg/ml) 100 mm dishes (Nunc, MA), treated with drug (10 min at 37°C), rinsed once and harvested (ice-cold 1xPBS, pH 7.2, supplemented with cOmplete protease inhibitor cocktail and PhosSTOP phosphatase inhibitor cocktail (Roche, IN) and 1 mM PMSF). Whole cell extracts were prepared in lysis buffer (in mM) Tris-HCl 500, pH 7.4, NaCl 1500, 2.5% deoxycholic acid, 10% NP-40, EDTA 10, PMSF 1, Na_3VO_4 1, NaF 1, supplemented with cOmplete protease and PhosSTOP phosphatase inhibitor cocktails, and processed for Western blot subject to the study inclusion criteria below: Cultures that were judged to be network functional by confocal were thus included in the analysis.

Confocal Ca^{2+} imaging of cortical and hippocampal neurons: The cells, cultured as above on confocal dishes, were incubated for 30 min at 37°C with the cell membrane-permeant calcium indicator Fluo-4 acetoxymethyl ester (Invitrogen, CA). The cells were imaged at room temperature in imaging buffer (in mM) NaCl 137, KCl 5, $CaCl_2$ 3, glucose 25, HEPES 10 in real time using a Zeiss Laser Scanning Microscope (LSM) 510, excitation 488 nm, emission 505-735 nm. Images were captured at 1.57 s

Downloaded from molpharm.aspetjournals.org at ASPET Journals on March 20, 2024

Molecular Pharmacology Fast Forward. Published on July 23, 2014 as DOI: 10.1124/mol.114.094128
This article has not been copyedited and formatted. The final version may differ from this version.

per frame using a 40x water immersion objective. Regions of interest were selected for morphologically identified cells using Zeiss Axiovert software to determine changes in fluorescence intensity with a dynamic range of 0-255. The effect of drug application was quantified as the ratio of peak fluorescence above baseline during saline vs drug application $\Delta F/F = [(F/Fo)drug - (F/Fo)baseline]$.

Both cortical and hippocampal neurons exhibited spontaneous sEPSCs, bursting firing patterns consistent with action potentials, and oscillations of firing rate indicative of effective synaptic local network function. Oscillatory network activity in cortical and hippocampal cultures that exceeded 20% of baseline average had to be excluded from use as it was not possible to identify a true baseline level of the F/F_0. Neuronal cultures were subject to three criteria for inclusion in the study: (1) ongoing network activity as judged by oscillatory fluctuations in F_0 with some spiking activity were required, however, as noted above, (2) the average baseline slow waves were within 20% of F_0, and (3) individual neurons were responsive to depolarization with 50 mM KCl (at least 40% over baseline).

In experiments designed for western blot analysis, sister cultures for each study group were first screened by confocal microscopy as described above. To validate the measurements, cortical cells were exposed 50 mM KCl resulting in a significant increase in pCREB (relative to CREB) of ~ 90% when compared to VEH ($p<0.05$, unpaired t-test). Experimental groups in which sister slices showed an increase in pCREB relative to CREB following 50 mM KCl treatment were determined to have passed the basic criteria for signal transduction, i.e., that pCREB could be formed by the cells, and thus the experimental group was included in the analysis. When any part of plating failed either

Downloaded from molpharm.aspetjournals.org at ASPET Journals on March 20, 2024

Molecular Pharmacology Fast Forward. Published on July 23, 2014 as DOI: 10.1124/mol.114.094128
This article has not been copyedited and formatted. The final version may differ from this version.

the network activity test or signal transduction test all parts of the experiment were excluded from analysis.

***Rat hippocampal brain slices*:** Adult male Sprague Dawley rats aged P16-P30 were housed at room temperature in a light-controlled room with free access to food and water. The rats were anesthetized using isoflurane and decapitated. The brain was removed during dissection, while the head was submerged in ice-cold (4-5°C) artificial cerebrospinal fluid (aCSF), which was oxygenated with a gas mixture of 95% O_2/5% CO_2.The aCSF contained (in mM): 2.5 KCl, 1.25 NaH_2PO_4, 10 $MgSO_4$, 0.5 $CaCl_2$, 234 sucrose, 11 glucose, and 26 $NaHCO_3$, pH = 7.4 (310 Osm). Hemisected coronal slices (400 μm) containing the hippocampus were cut on a Leica vibratome and transferred to a recording chamber containing oxygenated aCSF at room temperature. This aCSF contained (in mM): 126 NaCl, 2.5 KCl, 1.25 NaH_2PO_4, 1 $MgSO_4$, 2 $CaCl_2$, 10 glucose, and 26 $NaHCO_3$, pH = 7.4 (310 Osm). Brain slices were allowed to recover for 1 hour before recording/drug treatment and then placed in a submerged thermostat-controlled recording chamber (28-29°C), which was continuously perfused with oxygenated aCSF at a flow rate of 2 ml/min. Slices were perfused with VEH (aCSF + 0.05% DMSO), 50 pM PregS (50 pM PregS in VEH), or 50 mM KCl (aCSF containing 50 mM KCl) for 10 min. For measurement of paired pulse facilitation (PPF) to confirm slice health and intact hippocampal circuitry, we used current pulses (0.1 ms) at interstimulus intervals (ISIs) of 10, 50, and 100 ms. Field excitatory postsynaptic potentials (fEPSPs) were elicited by stimulating Schaffer collaterals using a platinum concentric bipolor stimulating electrode and recorded with a glass microelectrode filled with aCSF (~1 MΩ) placed in the stratum radiatum

Downloaded from molpharm.aspetjournals.org at ASPET Journals on March 20, 2024

Molecular Pharmacology Fast Forward. Published on July 23, 2014 as DOI: 10.1124/mol.114.094128
This article has not been copyedited and formatted. The final version may differ from this version.

of the CA1 region at a depth of about 100 µm. Data was acquired with EPC-9 patch-clamp amplifier (HEKA Electronics, Germany) and analyzed with Pulse-PulseFit software (version 8.11, HEKA Electronics).

Hippocampal slices that did not exhibit facilitation (slope of the second fEPSP was not larger than of first fEPSP for all three ISIs) and did not have a higher slope ratio for 50 ms ISI compared to the 10 and 100 ms ISIs, consistent with the residual Ca^{2+} hypothesis, were not judged to be network functional and thus not included in the analysis. The application of aCSF containing 50 mM KCl resulted in a significant increase in pCREB (relative to CREB) of 87.9% when compared to VEH ($p<0.05$, unpaired t-test). Experimental groups in which sister slices showed an increase in pCREB relative to CREB following 50 mM KCl treatment were determined to have passed the basic criteria for signal transduction and thus the experimental group was included in the analysis.

Hippocampal tissue dissected for western blot was frozen at -80°C, sonicated in ice cold phosphate buffered saline (PBS) solution (1 mM PMSF, protease+phosphatase inhibitors (Roche) in PBS) for 1 s, and centrifuged (1 s, 4,000 rpm, 5 min, 4°C). The pellet was resuspended in 50 µL of homogenization buffer (RIPA (Cell Signaling Technology, MA), 1 mM PMSF, protease+phosphatase inhibitors cocktail (Roche), 1 mM Na_3VO_4, 1 mM NaF). The resuspended pellet was incubated at 4°C for 15 min, centrifuged at 13,000 rpm for 10 min at 4°C, and the supernatant processed by Western blot.

Proteins were resolved under reducing conditions (100 mM DTT) using SDS-PAGE and transferred to nitrocellulose membranes (Invitrogen, CA). Membranes were

Downloaded from molpharm.aspetjournals.org at ASPET Journals on March 20, 2024

Molecular Pharmacology Fast Forward. Published on July 23, 2014 as DOI: 10.1124/mol.114.094128
This article has not been copyedited and formatted. The final version may differ from this version.

incubated in anti-sera raised against phospho-CREB (pCREB) or CREB (both 1:1000; Cell Signaling, MA) followed by incubation in HRP-conjugated secondary antibody (1:2000; Santa Cruz Biotechnology, CA). Blots were stripped and incubated in anti-sera raised against β-actin (1:30,000; Sigma-Aldrich, MO) followed by incubation in peroxidase-conjugated secondary antibody (1:15,000; Vector Laboratories, CA), and visualized using ECL Plus (GE Healthcare, WI).

Drugs: Steroids (Steraloids (RI)) were prepared as stock solutions in DMSO and diluted into imaging buffer (final [DMSO] = 0.05%). D(-)-2-amino-5-phosphonopentanoic acid (D-AP5), ifenprodil, MK-801, bicuculline (BIC), tetrodotoxin (TTX), diethylstilbestrol (DES), KN-93, and nifedipine were from Sigma-Aldrich (MO), Ro 25-6981 and BD 1063 were from Tocris (MO), 6-cyano-7-nitroquinoxaline-2,3-dione (CNQX) was from Abcam (MA), and U0126 was from EMD Millipore (MA).

Potency determinations: PregS like all hydrophobic molecules likely binds cellular components and surfaces in addition to degradation by sulfatases that may reduce the effective "free" concentration of ligand in solution. The potency for PregS of 2 pM could thus represent an upper limit.

Statistics: Except where otherwise noted, Tukey's multiple comparison test was used for all p values. When two comparisons were made the Student's t-test was used. The mean EC_{50} and 95% confidence limits (CI) for PregS induced-increase of $[Ca^{2+}]_i$ were estimated by nonlinear logistic regression using GraphPad Prism.

Results

We previously reported the phenomenon of delayed onset potentiation of the NMDAR response by PregS and that this was a Ca^{2+} dependent process that results in the

Downloaded from molpharm.aspetjournals.org at ASPET Journals on March 20, 2024

Molecular Pharmacology Fast Forward. Published on July 23, 2014 as DOI: 10.1124/mol.114.094128
This article has not been copyedited and formatted. The final version may differ from this version.

movement of functional receptors to the cell surface of cortical neurons and *Xenopus* oocytes stimulated via a non-canonical G-protein coupled mechanism (Kostakis *et al.*, 2013). Here we sought to determine whether the effect of PregS could exert functionally significant effects on excitatory synaptic transmission at physiological concentrations and couple to a downstream signal transduction mechanism associated with learning and memory.

Cortical neurons were loaded with the fluorescent Ca^{2+} indicator fluo-4 (Grienberger and Konnerth, 2012), imaged using confocal microscopy, and tested for the effect of various steroids with or without signal transduction inhibitors. A physiological concentration of PregS (50 pM) induces a transient elevation of F/Fo in the soma (**Fig. 1a-c**), indicating the existence of a high potency mechanism for increasing neuronal $[Ca^{2+}]_i$. PREG (50 pM) has no effect on $[Ca^{2+}]_i$, while the subsequent co-application of PregS (50 pM) + PREG (50 pM) increases $[Ca^{2+}]_i$ **(Fig. 1d).** 50 pM PregS also increases $[Ca^{2+}]_i$ in cultured hippocampal neurons but to a smaller magnitude (**Fig. 1e**). Dose-response analysis with PregS concentrations ranging from 500 fM to 5 nM yields an EC_{50} of 2 pM (**Fig. 2a**), which is about six orders of magnitude more potent than PregS (Wu *et al.*, 1991) as positive allosteric modulators of NMDA induced current.

NMDAR or AMPAR blockade by dAP5 or CNQX (Itazawa *et al.*, 1997) inhibits PregS-induced $[Ca^{2+}]_i$ increase (**Fig. 2c, d**) and an NR2B-specific antagonist, Ro 25-6981 (Fischer *et al.*, 1997), blocks PregS-induced increases in $[Ca^{2+}]_i$ with IC_{50} = 3 μM (**Fig. 2b**), The results are consistent with a requirement for excitatory NR2B subunit and AMPAR containing NMDAR-dependent synaptic activity upstream of the PregS induced increase in $[Ca^{2+}]_i$. Inhibition of 20 μM NMDA-induced $[Ca^{2+}]_i$ increase by the NR2B-

Downloaded from molpharm.aspetjournals.org at ASPET Journals on March 20, 2024

Molecular Pharmacology Fast Forward. Published on July 23, 2014 as DOI: 10.1124/mol.114.094128
This article has not been copyedited and formatted. The final version may differ from this version.

specific antagonist ifenprodil (IFEN) (Williams, 1993) was compared to inhibition of the 50 pM PregS-induced $[Ca^{2+}]_i$ increase by IFEN and Ro25-6981 (**Fig. 2b**). Whereas inhibition of the NMDA-induced $[Ca^{2+}]_i$ increase by IFEN was consistent with previous published findings (Church *et al.*, 1994), IFEN inhibits PregS-induced $[Ca^{2+}]_i$ increases with an IC_{50} = 10 pM, while Ro-256981 inhibits the PregS-induced $[Ca^{2+}]_i$ increase with IC_{50} = 3 μM, a 5-order of magnitude difference in potency. The difference in potency between IFEN inhibition of 50 pM PregS vs. 20 μM NMDA is consistent with the identification of a novel high affinity site for IFEN associated with the pM PregS binding site, suggesting a potential novel site of action for high potency IFEN modulation of NMDARs.

Modulation of NMDA-induced $[Ca^{2+}]_i$ by neuroactive steroids depends on geometry and charge and PREG, the uncharged precursor to PregS, does not modulate NMDAR function (Weaver *et al.*, 2000). PregHS, a synthetic chemical mimic of PregS with a succinate group substituted for the sulfate group at the C3 carbon, increases $[Ca^{2+}]_i$, indicating that the C3 negative charge (and its structure (sulfate vs. succinate)) is essential to activate PREG for high potency $[Ca^{2+}]_i$ increases **(Fig. 2e)**. A C5-6 double bond confers a planar structure to PregS. In contrast, pregnanolone sulfate (PAS) at 50 pM, a B-ring saturated steroid with a bent configuration, did not increase $[Ca^{2+}]_i$, indicating that the C5-C6 double bond is required for the high potency PregS-induced $[Ca^{2+}]_i$ increase **(Fig. 2e)**. The lack of effect of B-ring saturated steroids was confirmed by PAHS (50 pM), a chemical mimic of PAS with a negatively charged succinate group substituted for the C3 sulfate, which did not increase $[Ca^{2+}]_i$ **(Fig. 2e)**. Thus neither the reduced metabolite pregnanolone (PA) nor its downstream sulfated metabolites had any

Downloaded from molpharm.aspetjournals.org at ASPET Journals on March 20, 2024

Molecular Pharmacology Fast Forward. Published on July 23, 2014 as DOI: 10.1124/mol.114.094128
This article has not been copyedited and formatted. The final version may differ from this version.

effect on $[Ca^{2+}]_i$ at 50 pM steroid (**Fig. 2e**). Taken together, the results are consistent with a binding site for PregS-induced $[Ca^{2+}]_i$ increase that requires a negatively charged C3 group (sulfate > succinate) restricted to a planar pregnene and not a reduced pregnane metabolite.

Tetrodotoxin (TTX, 30 min) eliminated the PregS-induced $[Ca^{2+}]_i$ increase (**Fig. 3a**), demonstrating a requirement for NaV dependent neuronal activity (Romano-Silva *et al.*, 1994). This also indicates that PregS does not induce presynaptic Ca^{2+} influx coupled to glutamate release because this mechanism would not be blocked by TTX. Consistent with this mechanism, nifedipine blocks PregS $[Ca^{2+}]_i$ increases (**Fig. 3b**), indicating $Ca^{2+}{}_L$ activation and post-synaptic membrane depolarization is an obligatory step.

The sigma-R subtype 1 antagonist BD1063 (1 μM) (Matsumoto *et al.*, 1995) had no effect on PregS-induced $[Ca^{2+}]_i$ increases. DES, a store-operated calcium channel inhibitor (Zakharov *et al.*, 2004) does not block 50 pM PregS-induced $[Ca^{2+}]_i$ increases (**Fig. 3c,d**). PregS-induced $[Ca^{2+}]_i$ increase requires $Ca^{2+}{}_L$, and induces CREB phosphorylation (pCREB) in primary cultured cortical neurons and hippocampal brain slices (**Fig. 4a-c**). Brain slices were shown to be active via concomitant slice electrophysiology. Field recording electrophysiology demonstrated functional network activity, consistent with the hypothesis that the rapid effect of 50 pM PregS as an activator of CREB is mediated via systems level synaptic activity. These results above indicate that PregS induces pCREB, and may be associated with long-term changes in synaptic potentiation via $Ca^{2+}{}_L$ activity (Shaywitz and Greenberg, 1999).

The observation that PregS but not PREG increases $[Ca^{2+}]_i$ **(Fig. 2e)** demonstrates that the response requires a negative charge at C3 and B-ring saturation. To determine

Downloaded from molpharm.aspetjournals.org at ASPET Journals on March 20, 2024

Molecular Pharmacology Fast Forward. Published on July 23, 2014 as DOI: 10.1124/mol.114.094128
This article has not been copyedited and formatted. The final version may differ from this version.

whether the effect of PregS on pCREB exhibits similar structural specificity, the effects of PAS, PAHS, and PregHS were tested. Only PregHS reproduced the effect of PregS, confirming the requirement for B-ring saturation. In addition, neither dehydroepiandrosterone (DHEA) nor its sulfate ester, DHEAS, increased pCREB (**Fig. 4b**). This result indicates that while B-ring saturation is required, a C3 negative charge alone is not sufficient to confer neuroactive steroid-pCREB activity, and that additional structural constraints such as the length of the C-17 group may also play a role in PregS activation of pCREB.

Activation of glutamate receptors can lead to calmodulin (CaM) activation (Bading *et al.*, 1993) and subsequent CaM kinase II (CaMKII) phosphorylation of CREB (Fukunaga and Miyamoto, 2000). However, the CaMKII inhibitor KN93 (0.25 μM) (Sumi *et al.*, 1991) did not abolish PregS-induced increases in pCREB (**Fig. 5a**) Alternatively, the MAPK signaling pathway may be activated by NMDARs or by Ca^{2+} influx through Ca^{2+}_L (Thomas and Huganir, 2004); therefore, if activation of the MAPK pathway by either the NMDAR or Ca^{2+}_L is occurring during PregS application, blockade of the MAPK pathway would eliminate PregS increases in pCREB levels. Inhibition of MEK using U0126 (Favata *et al.*, 1998) blocks PregS-induced pCREB increases (**Fig 5b**). PregS also induces an increase in the ratio of phospho-ERK (pERK) to total ERK (**Fig. 5c**), demonstrating that PregS directly activates pERK. Together, these results indicate that PregS activation of the MAPK signaling pathway is required for PregS-elevation of pCREB levels.

If pCREB activation is a physiological consequence of PregS-induced $[Ca^{2+}]_i$ increase, the phenomenon should also depend on excitatory neurotransmission. To

Downloaded from molpharm.aspetjournals.org at ASPET Journals on March 20, 2024

Molecular Pharmacology Fast Forward. Published on July 23, 2014 as DOI: 10.1124/mol.114.094128
This article has not been copyedited and formatted. The final version may differ from this version.

determine if PregS-induced pCREB increases are dependent on action potentials the cultures were treated with TTX prior to PregS application, which eliminated PregS-induced elevations of pCREB (**Fig. 6a**). Synaptic NMDAR activation leads to increased pCREB, whereas extrasynaptic NMDAR activation leads to pCREB dephosphorylation (Hardingham *et al.*, 2002). We hypothesized that selective blockade of synaptic NMDARs should block the effect of PregS on pCREB while avoiding extrasynaptic NMDAR-mediated disinhibition of pCREB activation. Prior to PregS application, we blocked $GABA_A$Rs using bicuculline (BIC) that instantaneously induces synaptic glutamate release via disinhibition. The activated NMDARs were blocked with MK-801, leaving only extrasynaptic NMDARs activatable (Hardingham *et al.*, 2002). We determined that synaptic NMDAR inhibition blocked PregS-induced pCREB increases (**Fig. 6b**), indicating dependence upon synaptic but not extrasynaptic NMDAR activity.

The effects of PregS on excitatory synaptic transmission are modeled in **Figure 7**. PregS, acting either on presynaptic glutamate release or at post-synaptic receptors enhances NMDAR signaling and pCREB activation contingent upon a MAPK signal transduction pathway.

Discussion

PregS at μM concentrations enhances NMDA-induced membrane current (Wu *et al.*, 1991) and increases $[Ca^{2+}]_i$ (Irwin *et al.*, 1992); however, it is unlikely that PregS at micromolar concentrations occur naturally in widespread brain regions as bulk concentrations of PregS in rat and human brain occur at low-nM or sub-nM levels (Liere *et al.*, 2004). However, a recent study using an improved method of mass-spectrometry without solvolysis found bulk levels as high as 25 nM in rat hippocampus and 11 nM in

Downloaded from molpharm.aspetjournals.org at ASPET Journals on March 20, 2024

Molecular Pharmacology Fast Forward. Published on July 23, 2014 as DOI: 10.1124/mol.114.094128
This article has not been copyedited and formatted. The final version may differ from this version.

cortex (Rustichelli *et al.*, 2013). The ability of nerve terminals and glial cells to concentrate neurotransmitters and ions at local concentrations in large excess over bulk cellular levels is well established, leaving the question of synaptic function and modulation of synaptic function by PregS open.

Although reports of low brain levels of PregS have raised questions as to whether PregS modulation of NMDAR function occurs in vivo, the modulatory effects of PregS occurs in the striatum of awake rats at 10 nM, increasing DA overflow (Sadri-Vakili *et al.*, 2008). Moreover, efflux of [^{3}H]DA from striatal synaptosomes is enhanced by PregS at concentrations as low as 25 pM (Whittaker *et al.*, 2008). Notably, in both cases there is evidence for involvement of NMDARs.

We now report that PregS stimulates a NMDAR-dependent increase in $[Ca^{2+}]_i$ in cortical neurons with an EC_{50} of 2 pM. This concentration is well below the most sensitive detection limit reported for determination of PregS in rodent brain (~50 pM, (Jäntti *et al.*, 2010)), and suggests that endogenous PregS modulation of synaptic transmission could be occurring in rat brain.

We recently reported that PregS, at high nM to low μM concentrations, releases Ca^{2+} from intracellular stores in *Xenopus* oocytes expressing NR1/NR2A or NR1/NR2B receptors via a noncanonical mechanism that requires NMDARs but does not involve activation of the NMDAR ion channel (Kostakis *et al.*, 2013). Pharmacological evidence indicates that PregS-induced release of intracellular Ca^{2+} is mediated by G-protein coupled activation of phospholipase C. It is unclear whether the increase in neuronal $[Ca^{2+}]_i$ elicited by pM concentrations of PregS is related to that finding. In addition to the large difference in potency, the increase in $[Ca^{2+}]_i$ produced by in neurons by pM PregS

Downloaded from molpharm.aspetjournals.org at ASPET Journals on March 20, 2024

Molecular Pharmacology Fast Forward. Published on July 23, 2014 as DOI: 10.1124/mol.114.094128
This article has not been copyedited and formatted. The final version may differ from this version.

is dependent upon the involvement of Ca^{2+}_L, suggesting a role for entry of extracellular Ca^{2+}.

Whether the recognition site at which pM PregS acts to increase $[Ca^{2+}]_i$ is different from the site that μM PregS acts to potentiate the NMDA response (Jang *et al.*, 2004) remains a provocative question. Inhibition of increased $[Ca^{2+}]_i$ by 50 pM PregS by D-AP5, ifenprodil, and Ro 25-6981 strongly suggests involvement of NMDARs. The failure of CNQX to fully block the PregS-induced $[Ca^{2+}]_i$ increase indicates that membrane depolarization by AMPARs contributes, but is not an absolute requirement for NMDAR and Ca^{2+}_L-mediated PregS-induced increases in $[Ca^{+2}]_i$. There may be incomplete Mg^{2+} block of NMDARs or contribution by an additional ion channel activated by PregS.

The steroid structure-activity relationship for the PregS-induced $[Ca^{2+}]_i$ increase is consistent with that previously described for rapid allosteric modulation of NMDA-induced $[Ca^{2+}]_i$ increase by PregS (Weaver *et al.*, 2000), but the EC_{50} for PregS potentiation of $[Ca^{2+}]_i$ is over 6 orders of magnitude lower (higher potency), which argues for a distinct binding site. On the other hand, PregS is lipophilic and charged so the observed potency could be substantially enhanced if PregS accesses its recognition site from within or at the lipid bilayer.

This leaves the intriguing possibility that a single novel receptor might trigger diverse downstream cellular signaling events by coupling to NMDARs, GPCRs, and Ca^{2+} channels, leading to long-term changes in neuronal gene expression via CREB phosphorylation. PregS and PAHS increase $[Ca^{2+}]_i$ and pCREB but PREG, PA, PAS, and PAHS do not, consistent with the hypothesis that the same structural features (a

Downloaded from molpharm.aspetjournals.org at ASPET Journals on March 20, 2024

Molecular Pharmacology Fast Forward. Published on July 23, 2014 as DOI: 10.1124/mol.114.094128
This article has not been copyedited and formatted. The final version may differ from this version.

negative charge at C-3 and C-5,6 double bond) are required for both and linking the increase in $[Ca^{2+}]_i$ with the increase in pCREB.

The Ca^{2+} imaging and pCREB data are also consistent with a requirement for synaptic activity for high-potency PregS effects. If PregS were acting directly on presynaptic Ca^{2+}channels, TTX would not be expected to block the effect of PregS on Ca^{2+}. Blockade of the PregS-induced $[Ca^{2+}]_i$ increase by the NMDAR antagonist D-AP5, as well as inhibition of PregS-induced pCREB by blockade of synaptic NMDARs with BIC/MK-801, further support the hypothesis that PregS effects on Ca^{2+} and pCREB require synaptic activity. The $Ca^{2+}{}_L$ inhibitor nifedipine blocked PregS-induced increases in $[Ca^{2+}]_i$, consistent with the entry of extracellular Ca^{2+} via $Ca^{2+}{}_L$ activation leading to pCREB increases (Dolmetsch *et al.*, 2001). Although F/Fo remains slightly elevated after the initial increase in $[Ca^{2+}]$, the results do not support the co-involvement SOCC (Zakharov *et al.*, 2004) in the PregS response.

As there are numerous pathways by which pCREB is activated by extracellular signals (Shaywitz and Greenberg, 1999), we sought to determine which pathway is involved in PregS-induced pCREB. PregS was found to induce ERK phosphorylation, while inhibition of MAPK blocked PregS-induced pCREB, implicating the MAPK pathway in PregS-induced pCREB via modulation of synaptic transmission. Inhibition of CaMKII did not eliminate the effect of PregS, and the complete inhibition of the effect of PregS on pCREB by MAPK blockade virtually rules out other pathways leading to pCREB activation. 50 pM PregS is sufficient to activate CREB via an NR2B and Ca^{2+} contingent synaptic mechanism, a signal transduction mechanism known to be involved in LTP and cognition.

Downloaded from molpharm.aspetjournals.org at ASPET Journals on March 20, 2024

Molecular Pharmacology Fast Forward. Published on July 23, 2014 as DOI: 10.1124/mol.114.094128
This article has not been copyedited and formatted. The final version may differ from this version.

The data provide further support for the possible biological role of the neurosteroid PregS, acting at picomolar concentrations to intensify the intracellular response to glutamatergic signaling at synaptic, but not extra-synaptic, NMDA receptors (see Fig. 7 for summary). This adds a modulatory dimension to information processing via chemical signaling and a potential new pathway toward the therapeutics of neuropsychiatric disorders, such as schizophrenia. It is interesting to wonder whether the biological relevance of endogenous PregS to brain function may be a window on neurosteroid modulation of synaptic events that lead to enhanced cognitive performance.

Downloaded from molpharm.aspetjournals.org at ASPET Journals on March 20, 2024

Molecular Pharmacology Fast Forward. Published on July 23, 2014 as DOI: 10.1124/mol.114.094128
This article has not been copyedited and formatted. The final version may differ from this version.

Authorship Contributions:

Participated in research design: Smith, Farb, Martin, Russek, Gibbs, Sugunan

Conducted experiments: Smith, Martin, Sugunan

Performed data analysis: Smith, Martin, Sugunan

Wrote or contributed to the writing of the manuscript: Smith, Farb, Gibbs, and Russek

Downloaded from molpharm.aspetjournals.org at ASPET Journals on March 20, 2024

Molecular Pharmacology Fast Forward. Published on July 23, 2014 as DOI: 10.1124/mol.114.094128
This article has not been copyedited and formatted. The final version may differ from this version.

References

Ahmed T, and Frey JU (2005) Plasticity-specific phosphorylation of CaMKII, MAP-kinases and CREB during late-LTP in rat hippocampal slices in vitro. *Neuropharmacology* **49**:477–492.

Akwa Y, Ladurelle N, Covey DF, and Baulieu EE (2001) The synthetic enantiomer of pregnenolone sulfate is very active on memory in rats and mice, even more so than its physiological neurosteroid counterpart: distinct mechanisms? *Proc Natl Acad Sci U S A* **98**:14033–14037.

Bading H, Ginty DD, and Greenberg ME (1993) Regulation of gene expression in hippocampal neurons by distinct calcium signaling pathways. *Science (80-)* **260**:181–186.

Bibb JA, Mayford MR, Tsien JZ, and Alberini CM (2010) Cognition enhancement strategies. *J Neurosci* **30**:14987–14992.

Bourtchuladze R, Frenguelli B, Blendy J, Cioffi D, Schutz G, and Silva AJ (1994) Deficient long-term memory in mice with a targeted mutation of the cAMP-responsive element-binding protein. *Cell* **79**:59–68.

Chen L, Miyamoto Y, Furuya K, Mori N, and Sokabe M (2007) PREGS induces LTP in the hippocampal dentate gyrus of adult rats via the tyrosine phosphorylation of NR2B coupled to ERK/CREB [corrected] signaling. *J Neurophysiol* **98**:1538–1548.

Church J, Fletcher EJ, Baxter K, and MacDonald JF (1994) Blockade by ifenprodil of high voltage-activated Ca2+ channels in rat and mouse cultured hippocampal

Downloaded from molpharm.aspetjournals.org at ASPET Journals on March 20, 2024

Molecular Pharmacology Fast Forward. Published on July 23, 2014 as DOI: 10.1124/mol.114.094128
This article has not been copyedited and formatted. The final version may differ from this version.

pyramidal neurones: comparison with N-methyl-D-aspartate receptor antagonist actions. *Br J Pharmacol* **113**:499–507.

Colbert CM, and Johnston D (1996) Axonal action-potential initiation and Na+ channel densities in the soma and axon initial segment of subicular pyramidal neurons. *J Neurosci* **16**:6676–6686.

Collingridge GL, Volianskis A, Bannister N, France G, Hanna L, Mercier M, Tidball P, Fang G, Irvine MW, Costa BM, Monaghan DT, Bortolotto ZA, Molnár E, Lodge D, and Jane DE (2013) The NMDA receptor as a target for cognitive enhancement. *Neuropharmacology* **64**:13–26.

Coyle JT (2006) Glutamate and Schizophrenia: Beyond the Dopamine Hypothesis. *Cell Mol Neurobiol* **26**:365–384.

Darnaudéry M, Pallarès M, Piazza PV, Le Moal M, and Mayo W (2002) The neurosteroid pregnenolone sulfate infused into the medial septum nucleus increases hippocampal acetylcholine and spatial memory in rats. *Brain Res* **951**:237–242.

Dolmetsch RE, Pajvani U, Fife K, Spotts JM, and Greenberg ME (2001) Signaling to the nucleus by an L-type calcium channel-calmodulin complex through the MAP kinase pathway. *Science (80-)* **294**:333–339.

Favata MF, Horiuchi KY, Manos EJ, Daulerio AJ, Stradley DA, Feeser WS, Van Dyk DE, Pitts WJ, Earl RA, Hobbs F, Copeland RA, Magolda RL, Scherle PA, and Trzaskos JM (1998) Identification of a novel inhibitor of mitogen-activated protein kinase kinase. *J Biol Chem* **273**:18623–18632.

Fischer G, Mutel V, Trube G, Malherbe P, Kew JN, Mohacsi E, Heitz MP, and Kemp JA (1997) Ro 25-6981, a highly potent and selective blocker of N-methyl-D-aspartate

Downloaded from molpharm.aspetjournals.org at ASPET Journals on March 20, 2024

Molecular Pharmacology Fast Forward. Published on July 23, 2014 as DOI: 10.1124/mol.114.094128
This article has not been copyedited and formatted. The final version may differ from this version.

receptors containing the NR2B subunit. Characterization in vitro. *J Pharmacol Exp Ther* **283**:1285–1292.

Flood JF, Morley JE, and Roberts E (1995) Pregnenolone sulfate enhances post-training memory processes when injected in very low doses into limbic system structures: the amygdala is by far the most sensitive. *Proc Natl Acad Sci U S A* **92**:10806–10810.

Fukunaga K, and Miyamoto E (2000) A working model of CaM kinase II activity in hippocampal long-term potentiation and memory. *Neurosci Res* **38**:3–17.

Gibbs TT, Russek SJ, and Farb DH (2006) Sulfated steroids as endogenous neuromodulators. *Pharmacol Biochem Behav* **84**:555–567.

Grienberger C, and Konnerth A (2012) Imaging calcium in neurons. *Neuron* **73**:862–885.

Hardingham GE, Fukunaga Y, and Bading H (2002) Extrasynaptic NMDARs oppose synaptic NMDARs by triggering CREB shut-off and cell death pathways. *Nat Neurosci* **5**:405–414.

Irwin RP, Maragakis NJ, Rogawski MA, Purdy RH, Farb DH, and Paul SM (1992) Pregnenolone sulfate augments NMDA receptor mediated increases in intracellular Ca2+ in cultured rat hippocampal neurons. *Neurosci Lett* **141**:30–34.

Itazawa SI, Isa T, and Ozawa S (1997) Inwardly rectifying and Ca2+-permeable AMPA-type glutamate receptor channels in rat neocortical neurons. *J Neurophysiol* **78**:2592–2601.

Jang M-KK, Mierke DF, Russek SJ, and Farb DH (2004) A steroid modulatory domain on NR2B controls N-methyl-D-aspartate receptor proton sensitivity. *Proc Natl Acad Sci U S A* **101**:8198–8203.

Downloaded from molpharm.aspetjournals.org at ASPET Journals on March 20, 2024

Molecular Pharmacology Fast Forward. Published on July 23, 2014 as DOI: 10.1124/mol.114.094128
This article has not been copyedited and formatted. The final version may differ from this version.

Jäntti SE, Tammimäki A, Raattamaa H, Piepponen P, Kostiainen R, and Ketola RA (2010) Determination of steroids and their intact glucuronide conjugates in mouse brain by capillary liquid chromatography-tandem mass spectrometry. *Anal Chem* **82**:3168–3175.

Javitt DC (2007) Glutamate and Schizophrenia: Phencyclidine, N-Methyl-d-Aspartate Receptors, and Dopamine-Glutamate Interactions. *Int Rev Neurobiol 78:69-108.*

Kostakis E, Smith C, Jang M-KK, Martin SC, Richards KG, Russek SJ, Gibbs TT, and Farb DH (2013) The Neuroactive Steroid Pregnenolone Sulfate Stimulates Trafficking of Functional NMDA Receptors to the Cell Surface via a Non-Canonical G-Protein and Ca++ Dependent Mechanism. *Mol Pharmacol* **84**:261-74.

Kreinin A, Bawakny N, and Ritsner MS (2014) Adjunctive pregnenolone ameliorates the cognitive deficits in recent-onset schizophrenia. *Clin Schizophr Relat Psychoses* 1–31.

Liere P, Pianos A, Eychenne B, Cambourg A, Liu S, Griffiths W, Schumacher M, Sjövall J, and Baulieu E-E (2004) Novel lipoidal derivatives of pregnenolone and dehydroepiandrosterone and absence of their sulfated counterparts in rodent brain. *J Lipid Res* **45**:2287–302.

Malayev A, Gibbs TT, and Farb DH (2002) Inhibition of the NMDA response by pregnenolone sulphate reveals subtype selective modulation of NMDA receptors by sulphated steroids. *Br J Pharmacol* **135**:901–909.

Mameli M, Carta M, Partridge LD, and Valenzuela CF (2005) Neurosteroid-induced plasticity of immature synapses via retrograde modulation of presynaptic NMDA receptors. *J Neurosci* **25**:2285–2294.

Downloaded from molpharm.aspetjournals.org at ASPET Journals on March 20, 2024

Molecular Pharmacology Fast Forward. Published on July 23, 2014 as DOI: 10.1124/mol.114.094128
This article has not been copyedited and formatted. The final version may differ from this version.

Marx CE, Keefe RSE, Buchanan RW, Hamer RM, Kilts JD, Bradford DW, Strauss JL, Naylor JC, Payne VM, Lieberman JA, Savitz AJ, Leimone LA, Dunn L, Porcu P, Morrow AL, and Shampine LJ (2009) Proof-of-concept trial with the neurosteroid pregnenolone targeting cognitive and negative symptoms in schizophrenia. *Neuropsychopharmacology* **34**:1885–1903.

Marx CE, Shampine LJ, Duncan GE, VanDoren MJ, Grobin AC, Massing MW, Madison RD, Bradford DW, Butterfield MI, Lieberman JA, and Morrow AL (2006) Clozapine markedly elevates pregnenolone in rat hippocampus, cerebral cortex, and serum: candidate mechanism for superior efficacy? *Pharmacol Biochem Behav* **84**:598–608.

Matsumoto RR, Bowen WD, Tom MA, Vo VN, Truong DD, and De Costa BR (1995) Characterization of two novel sigma receptor ligands: antidystonic effects in rats suggest sigma receptor antagonism. *Eur J Pharmacol* **280**:301–310.

Mayo W, Dellu F, Robel P, Cherkaoui J, Le Moal M, Baulieu EE, and Simon H (1993) Infusion of neurosteroids into the nucleus basalis magnocellularis affects cognitive processes in the rat. *Brain Res* **607**:324–328.

Millan MJ (2005) N-Methyl-D-aspartate receptors as a target for improved antipsychotic agents: novel insights and clinical perspectives. *Psychopharmacology (Berl)* **179**:30–53.

Naylor JC, Hulette CM, Steffens DC, Shampine LJ, Ervin JF, Payne VM, Massing MW, Kilts JD, Strauss JL, Calhoun PS, Calnaido RP, Blazer DG, Lieberman JA, Madison RD, and Marx CE (2008) Cerebrospinal fluid dehydroepiandrosterone levels are correlated with brain dehydroepiandrosterone levels, elevated in Alzheimer's

Downloaded from molpharm.aspetjournals.org at ASPET Journals on March 20, 2024

Molecular Pharmacology Fast Forward. Published on July 23, 2014 as DOI: 10.1124/mol.114.094128
This article has not been copyedited and formatted. The final version may differ from this version.

disease, and related to neuropathological disease stage. *J Clin Endocrinol Metab* **93**:3173–3178.

Park-Chung M, Wu FS, Purdy RH, Malayev AA, Gibbs TT, and Farb DH (1997) Distinct sites for inverse modulation of N-methyl-D-aspartate receptors by sulfated steroids. *Mol Pharmacol* **52**:1113–1123.

Petit GH, Tobin C, Krishnan K, Moricard Y, Covey DF, Rondi-Reig L, and Akwa Y (2011) Pregnenolone sulfate and its enantiomer: differential modulation of memory in a spatial discrimination task using forebrain NMDA receptor deficient mice. *Eur Neuropsychopharmacol* **21**:211–215.

Plescia F, Sardo P, Rizzo V, Cacace S, Marino RAM, Brancato A, Ferraro G, Carletti F, and Cannizzaro C (2013) Pregnenolone sulphate enhances spatial orientation and object discrimination in adult male rats: evidence from a behavioural and electrophysiological study. *Behav Brain Res* 1–9.

Ritsner MS, Bawakny H, and Kreinin A (2014) Pregnenolone treatment reduces severity of negative symptoms in recent-onset schizophrenia: An 8-week, double-blind, randomized add-on two-center trial. *Psychiatry Clin Neurosci*, doi: 10.1111/pcn.12150.

Ritsner MS, Gibel A, Shleifer T, Boguslavsky I, Zayed A, Maayan R, Weizman A, and Lerner V (2010) Pregnenolone and dehydroepiandrosterone as an adjunctive treatment in schizophrenia and schizoaffective disorder: an 8-week, double-blind, randomized, controlled, 2-center, parallel-group trial. *J Clin Psychiatry* **71**:1351–1362.

Downloaded from molpharm.aspetjournals.org at ASPET Journals on March 20, 2024

Molecular Pharmacology Fast Forward. Published on July 23, 2014 as DOI: 10.1124/mol.114.094128
This article has not been copyedited and formatted. The final version may differ from this version.

Romano-Silva MA, Gomez M V, and Brammer MJ (1994) Modulation of Ca(2+)-stimulated glutamate release from synaptosomes by Na+ entry through tetrodotoxin-sensitive channels. *Biochem J* **304 (Pt 2)**:353–357.

Rujescu D, Bender A, Keck M, Hartmann AM, Ohl F, Raeder H, Giegling I, Genius J, McCarley RW, Möller HJ, and Grunze H (2006) A pharmacological model for psychosis based on N-methyl-D-aspartate receptor hypofunction: molecular, cellular, functional and behavioral abnormalities. *Biol Psychiatry* **59**:721–729.

Russek SJ, Bandyopadhyay S, and Farb DH (2000) An initiator element mediates autologous downregulation of the human type A gamma -aminobutyric acid receptor beta 1 subunit gene. *Proc Natl Acad Sci U S A* **97**:8600–8605.

Rustichelli C, Pinetti D, Lucchi C, Ravazzini F, and Puia G (2013) Simultaneous determination of pregnenolone sulphate, dehydroepiandrosterone and allopregnanolone in rat brain areas by liquid chromatography-electrospray tandem mass spectrometry. *J Chromatogr B Anal Technol Biomed Life Sci* **930**:62–69.

Sadri-Vakili G, Janis GC, Pierce RC, Gibbs TT, and Farb DH (2008) Nanomolar concentrations of pregnenolone sulfate enhance striatal dopamine overflow in vivo. *J Pharmacol Exp Ther* **327**:840–5.

Schumacher M, Liere P, Akwa Y, Rajkowski K, Griffiths W, Bodin K, Sj\Hovall J, and Baulieu E-E-. E (2008) Pregnenolone sulfate in the brain: a controversial neurosteroid. *Neurochem Int* **52**:522–540.

Shaywitz AJ, and Greenberg ME (1999) CREB: a stimulus-induced transcription factor activated by a diverse array of extracellular signals. *Annu Rev Biochem* **68**:821–861.

Downloaded from molpharm.aspetjournals.org at ASPET Journals on March 20, 2024

Molecular Pharmacology Fast Forward. Published on July 23, 2014 as DOI: 10.1124/mol.114.094128
This article has not been copyedited and formatted. The final version may differ from this version.

Sliwinski A, Monnet FP, Schumacher M, and Morin-Surun MP (2004) Pregnenolone sulfate enhances long-term potentiation in CA1 in rat hippocampus slices through the modulation of N-methyl-D-aspartate receptors. *J Neurosci Res* **78**:691–701.

Sumi M, Kiuchi K, Ishikawa T, Ishii A, Hagiwara M, Nagatsu T, and Hidaka H (1991) The newly synthesized selective Ca2+/calmodulin dependent protein kinase II inhibitor KN-93 reduces dopamine contents in PC12h cells. *Biochem Biophys Res Commun* **181**:968–975.

Thomas GM, and Huganir RL (2004) MAPK cascade signalling and synaptic plasticity. *Nat Rev Neurosci* **5**:173–183.

Vallée M, Mayo W, Darnaudéry M, Corpéchot C, Young J, Koehl M, Le Moal M, Baulieu EE, Robel P, and Simon H (1997) Neurosteroids: deficient cognitive performance in aged rats depends on low pregnenolone sulfate levels in the hippocampus. *Proc Natl Acad Sci U S A* **94**:14865–14870.

Vallée M, Vitiello S, Bellocchio L, Hébert-Chatelain E, Monlezun S, Martin-Garcia E, Kasanetz F, Baillie GL, Panin F, Cathala A, Roullot-Lacarrière V, Fabre S, Hurst DP, Lynch DL, Shore DM, Deroche-Gamonet V, Spampinato U, Revest J-M, Maldonado R, Reggio PH, Ross R a, Marsicano G, and Piazza PV (2014) Pregnenolone can protect the brain from cannabis intoxication. *Science* **343**:94–8.

Wagner TFJ, Loch S, Lambert S, Straub I, Mannebach S, Lis A, Flockerzi V, Philipp SE, and Oberwinkler J (2008) Transient receptor potential M3 channels are ionotropic steroid receptors in pancreatic β cells. *Cell* **10**:1421-30.

Weaver CE, Land MB, Purdy RH, Richards KG, Gibbs TT, and Farb DH (2000) Geometry and charge determine pharmacological effects of steroids on N-methyl-D-

Downloaded from molpharm.aspetjournals.org at ASPET Journals on March 20, 2024

Molecular Pharmacology Fast Forward. Published on July 23, 2014 as DOI: 10.1124/mol.114.094128
This article has not been copyedited and formatted. The final version may differ from this version.

aspartate receptor-induced Ca(2+) accumulation and cell death. *J Pharmacol Exp Ther* **293**:747–754.

Weill-Engerer S, David J-PP, Sazdovitch V, Liere P, Eychenne B, Pianos A, Schumacher M, Delacourte A, Baulieu E-EE, and Akwa Y (2002) Neurosteroid quantification in human brain regions: comparison between Alzheimer's and nondemented patients. *J Clin Endocrinol Metab* **87**:5138–5143.

Whittaker MT, Gibbs TT, and Farb DH (2008) Pregnenolone sulfate induces NMDA receptor dependent release of dopamine from synaptic terminals in the striatum. *J Neurochem* **107**:510–521.

Williams K (1993) Ifenprodil discriminates subtypes of the N-methyl-D-aspartate receptor: selectivity and mechanisms at recombinant heteromeric receptors. *Mol Pharmacol* **44**:851–859.

Wu FS, Gibbs TT, and Farb DH (1991) Pregnenolone sulfate: a positive allosteric modulator at the N-methyl-D-aspartate receptor. *Mol Pharmacol* **40**:333–336.

Zakharov SI, Smani T, Dobrydneva Y, Monje F, Fichandler C, Blackmore PF, and Bolotina VM (2004) Diethylstilbestrol is a potent inhibitor of store-operated channels and capacitative Ca(2+) influx. *Mol Pharmacol* **66**:702–707.

Downloaded from molpharm.aspetjournals.org at ASPET Journals on March 20, 2024

Molecular Pharmacology Fast Forward. Published on July 23, 2014 as DOI: 10.1124/mol.114.094128
This article has not been copyedited and formatted. The final version may differ from this version.

Footnotes

Acknowledgements: This work was supported by the National Institutes of Health, National Institute of Mental Health [Grant R01MH049469] to DHF and the National Institute of General Medical Sciences grants [T32GM008541] to DHF.

Reprint requests: David H. Farb, Ph.D., Department of Pharmacology & Experimental Therapeutics, Boston University School of Medicine, 72 East Concord St., Boston MA 02118, dfarb@bu.edu

Downloaded from molpharm.aspetjournals.org at ASPET Journals on March 20, 2024

Molecular Pharmacology Fast Forward. Published on July 23, 2014 as DOI: 10.1124/mol.114.094128
This article has not been copyedited and formatted. The final version may differ from this version.

Figure Legends

Fig. 1. Picomolar concentrations of PregS increase $[Ca^{2+}]_i$ in primary cultured cortical neurons. (A) Phase-contrast **(left)**, fluorescence **(middle)** and merged **(right)** image of a field of cortical neurons. **(B)** Before (**top**, 0 s) and after (**bottom**, 19 s) application of 50 pM PregS. Regions of interest defined morphologically as neuronal cell bodies are outlined in white. **(C)** Mean ± SEM fluorescence intensity normalized to average initial intensity of the same cell (F/F_o) for 3 neurons in (B). (**D**) Baseline Ca^{2+} fluorescence is shown in the (**left**) trace. 50 pM PREG does not increase $[Ca^{2+}]_I$ **(middle trace)**, while a subsequent application of 50 pM PregS in the presence of 50 pM PREG increases $[Ca^{2+}]_i$. (**right trace)** (Mean ± SEM, 30 neurons). (**E**) 50 pM PregS increases $[Ca^{2+}]_i$ in primary cultured hippocampal neurons. Scale bar for (**A**, **B**): 10μm.

Fig. 2. PregS induces a $[Ca^{2+}]_i$ increase in a dose-dependent and structure-specific manner. (**A**) Effect of PregS on levels of $[Ca^{2+}]_i$ (mean ± SEM) in monolayers of primary cultured cortical neurons. Concentration-response data was fit using nonlinear regression. Fitted values for the concentration-response curve include EC_{50} = 2 pM (indicated on the y-axis by green arrowhead). 95% confidence interval range: 1 – 5 pM, Hill slope = 0.7 ± 0.2, Emax = 0.45 ± 0.03. **(B)** IFEN displays high potency inhibition of PregS-induced $[Ca^{+2}]_i$ signal**.** The dose-inhibition curve for 50 pM PregS in the presence of IFEN (green circle, IC_{50} = 10 pM, 95% CI 6-17 pM) or Ro-256981 (green triangle, IC_{50} = 3 μM , 95% CI 0.2-49 mM), and NMDA (20μM) in the presence of IFEN (blue square, IC_{50} = 524 nM (95% CI 82 nM - 3350 nM). Results are normalized to PregS (50 pM) or NMDA (20 μM) controls in the absence of antagonist and fit using nonlinear regression. (n) =

Downloaded from molpharm.aspetjournals.org at ASPET Journals on March 20, 2024

Molecular Pharmacology Fast Forward. Published on July 23, 2014 as DOI: 10.1124/mol.114.094128
This article has not been copyedited and formatted. The final version may differ from this version.

number of cells. (**C**) D-AP5 (100 μM) an NMDAR antagonist inhibited the 50 pM PregS effect while (**D**) CNQX (2.5 μM) an AMPAR antagonist partially inhibited F/F_o. (**E**) Structural specificity of neuroactive steroid-induced $[Ca^{2+}]_i$ signal**.** All compounds were tested at 50 pM. One-way ANOVA $p<0.0001$ between all groups and Student's t-test (***$p<0.0001$, **$p<0.01$, (n.s.) not significant $p > 0.05$). PREG, PA, PAHS and PAS ($p > 0.05$, not shown). (n) = number of cells tested

Fig. 3. 50 pM PregS-induced $[Ca^{2+}]_i$ increase requires presynaptic action potentials, Ca^{2+}_L and NMDAR activation Primary cortical cultures were pretreated with drug at the indicated concentration or Veh for 30 min prior to acute application of 50 pM PregS ± drug and F/F_o measured. F/F_o was: **(A)** inhibited by TTX (1μM) the sodium channel (NaV) blocker (**B**) inhibited by nifedipine (NIF, 10 μM) the Ca^{2+}_L (CaV) inhibitor, but (**C**) not clearly inhibited by DES (100 nM) an SOCC inhibitor, or (**D**) BD1063 (1 μM) a sigma receptor (σR) antagonist. In (**A-D**) one-way ANOVA $p<0.05$ for all groups tested and post-hoc with Tukey's (*$p < 0.05$, **$p < 0.01$, ***$p < 0.001$). n.s. for (**A**) $p = 0.3$, (**B**) $p=0.6$, (**C**) $p=0.1$, (**D**) $p=0.2$.

Fig. 4. 50 pM PregS increases pCREB in primary cortical neurons and in hippocampal brain slice (**A)** Cortical neurons were treated with 0.05% DMSO (VEH) or PregS (50 pM) for 10 min at 37°C. Proteins were separated by SDS-PAGE followed by immunoblot with antibodies raised against pCREB or CREB. **(B)** Structural specificity of sulfated steroid pCREB induction (in primary cortical neurons)**.** Neurons were treated

Downloaded from molpharm.aspetjournals.org at ASPET Journals on March 20, 2024

Molecular Pharmacology Fast Forward. Published on July 23, 2014 as DOI: 10.1124/mol.114.094128
This article has not been copyedited and formatted. The final version may differ from this version.

with steroids as indicated, all at 50 pM concentration. Of steroids tested, only PregS and PHS increased pCREB. Comparison with one-way ANOVA $p < 0.05$ between all groups; post-hoc: *$p < 0.05$ vs. VEH, **$p < 0.01$ vs. VEH, #$p < 0.01$ vs. PregS). (n) = number of independent cultures. (**C**) 50 pM PregS increases pCREB in hippocampal slice by 65 ± 27% (*$p < 0.05$, Student's unpaired t-test). (n) = number of brain slices.

Fig. 5. 50 pM PregS increases pCREB via a MAPK signaling pathway (**A**) Representative pCREB and CREB protein bands following 30 min pretreatment with KN93 (250 nM) followed by 10 min 50 pM PregS treatment of primary cultured neurons. (**B**) Pretreatment for 30 min with the MEK1/MEK2 inhibitor U0126 (20 μM) prevents 50 pM PregS-induced pCREB increases. In (**A**) and (**B**), one-way ANOVA: $p < 0.05$ between all groups, post-hoc comparison: *$p < 0.05$ vs. VEH, #$p < 0.05$, ##$p < 0.01$ vs. PregS, (**C**) 50 pM PregS increases pERK. Treatments were as in (**A**), 50 pM PregS induces a 42 ± 12% increase in pERK. Pair-wise comparisons were performed with students t-test. (*$p < 0.05$). (n) = number of independent cultures.

Fig. 6. Inhibition of presynaptic action potentials blocks 50 pM PregS-induced pCREB (**A**) Primary cortical cultures were pretreated with TTX (1μM) or control for 30 min prior to a 10 min application of 50 pM PregS ± TTX. TTX eliminates PregS induced pCREB increase. Comparison by one-way ANOVA: $p < 0.05$ between all groups, post hoc comparison: *$p < 0.05$ (**B**) Synaptic NMDAR blockade by BIC (50 μM) and MK-801 (10μM) prevents 50 pM PregS activation of CREB. One-way ANOVA: $p < 0.05$

Downloaded from molpharm.aspetjournals.org at ASPET Journals on March 20, 2024

Molecular Pharmacology Fast Forward. Published on July 23, 2014 as DOI: 10.1124/mol.114.094128
This article has not been copyedited and formatted. The final version may differ from this version.

between all groups, pair-wise comparisons (Student's t-test): *$p < 0.05$. (n) = number of independent cultures.

Fig. 7. **Schematic illustrating pathways that may underlie pM PregS-induced $[Ca^{2+}]_i$ and pCREB increases.** Diagram illustrates 50 pM PregS-stimulated increase in $[Ca^{2+}]_i$ via voltage gated Na^+ channels, NMDARs and $Ca^{2+}{}_L$, and 50 pM PregS-induced pCREB increases via synaptic NMDAR and ERK activation. Inhibitors used in the study are in bold. *KN93 did not inhibit PregS-induced pCREB increases.

Downloaded from molpharm.aspetjournals.org at ASPET Journals on March 20, 2024

Molecular Pharmacology Fast Forward. Published on July 23, 2014 as DOI: 10.1124/mol.114.094128
This article has not been copyedited and formatted. The final version may differ from this version.

Figure 1

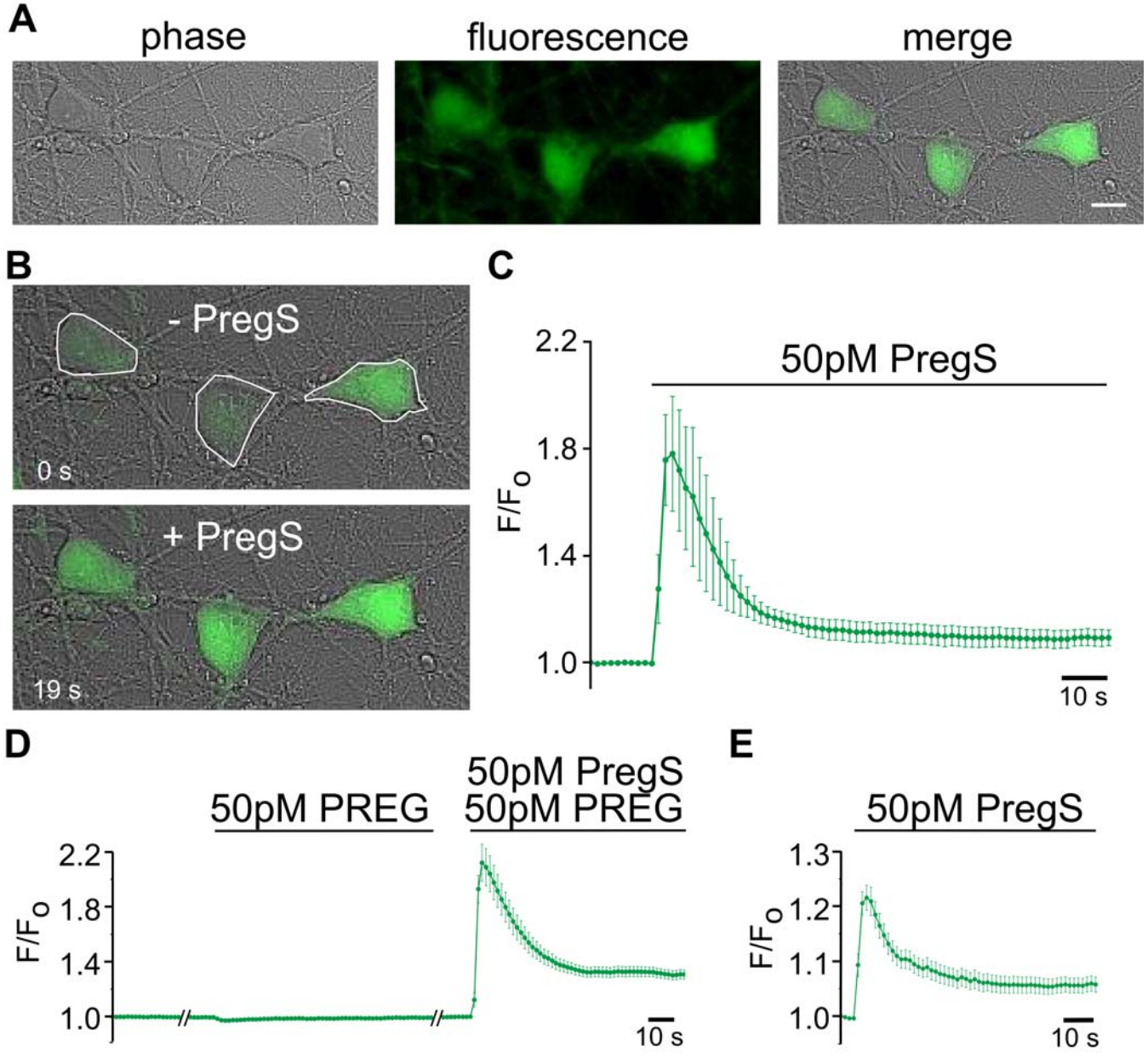

Downloaded from molpharm.aspetjournals.org at ASPET Journals on March 20, 2024

Molecular Pharmacology Fast Forward. Published on July 23, 2014 as DOI: 10.1124/mol.114.094128
This article has not been copyedited and formatted. The final version may differ from this version.

Figure 2

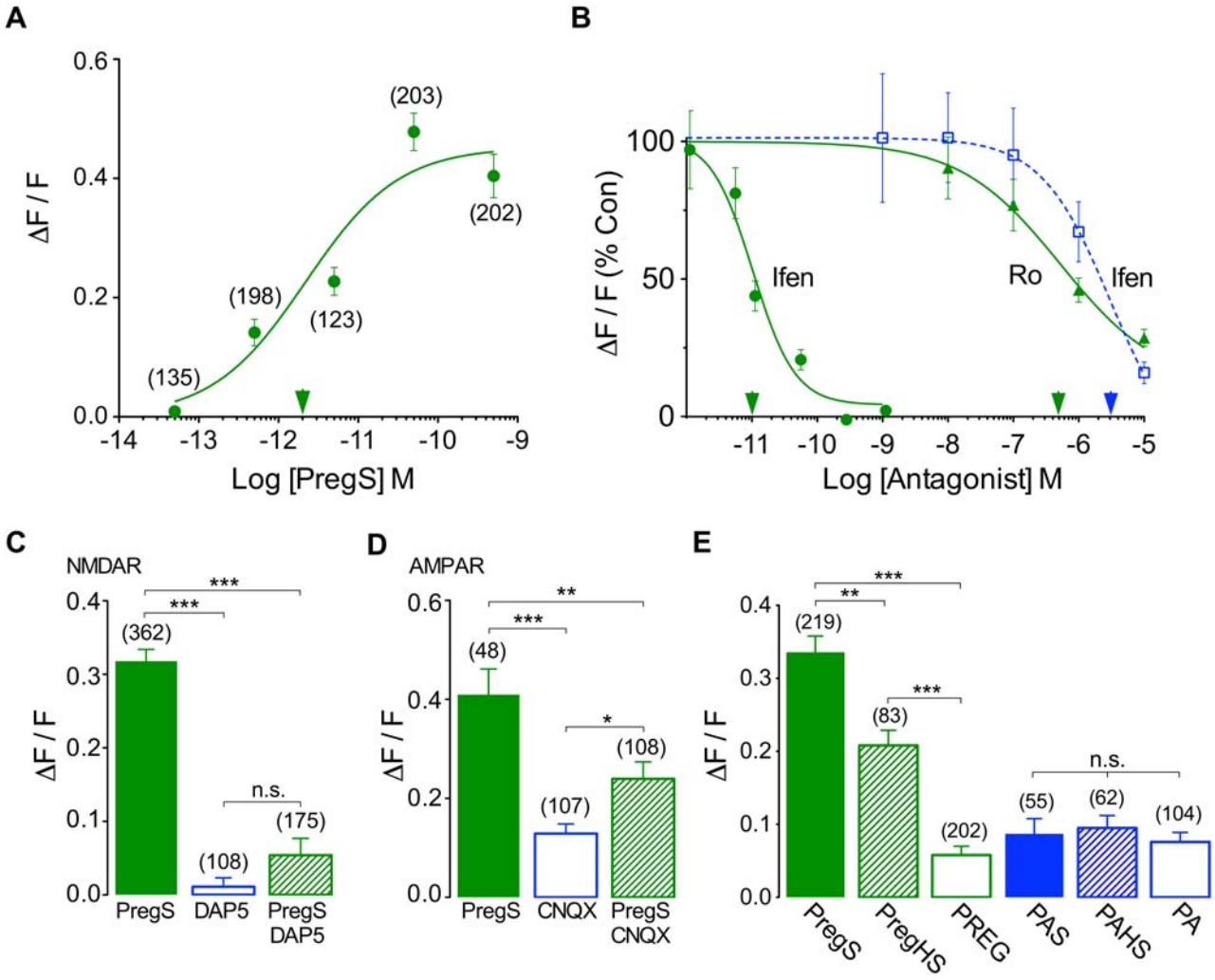

Downloaded from molpharm.aspetjournals.org at ASPET Journals on March 20, 2024

Molecular Pharmacology Fast Forward. Published on July 23, 2014 as DOI: 10.1124/mol.114.094128
This article has not been copyedited and formatted. The final version may differ from this version.

Figure 3

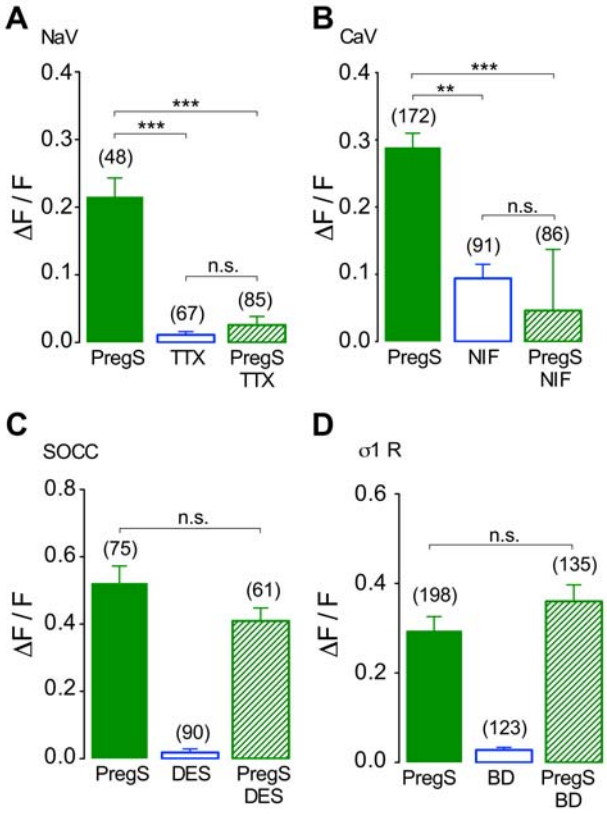

Downloaded from molpharm.aspetjournals.org at ASPET Journals on March 20, 2024

Molecular Pharmacology Fast Forward. Published on July 23, 2014 as DOI: 10.1124/mol.114.094128
This article has not been copyedited and formatted. The final version may differ from this version.

Figure 4

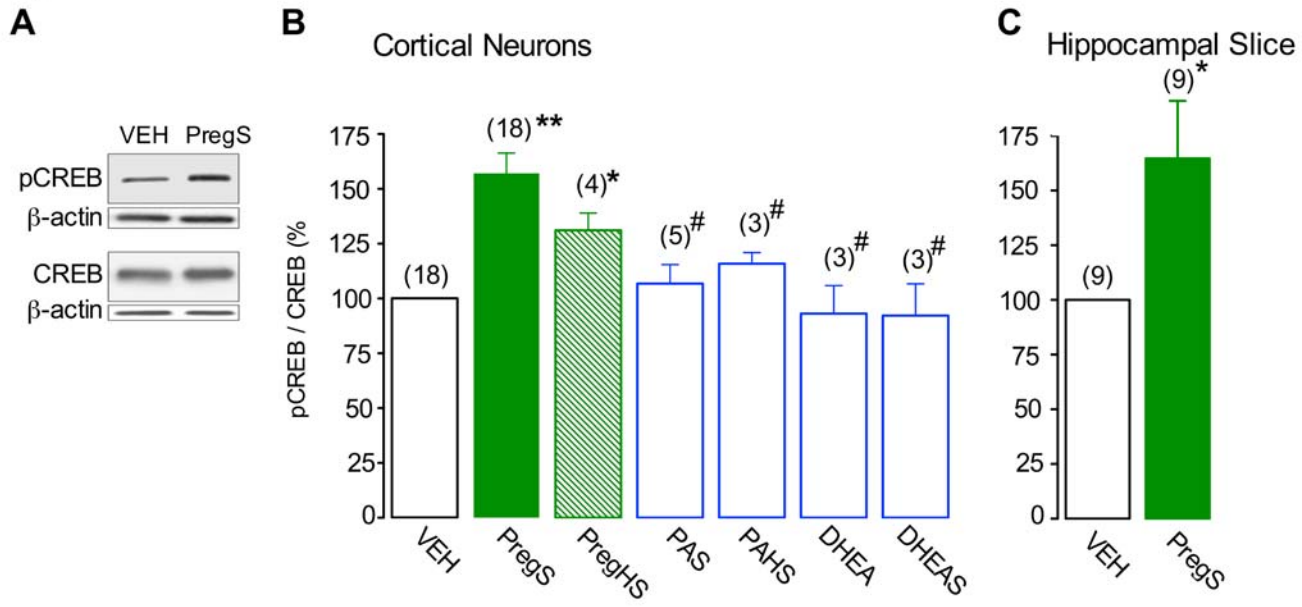

Downloaded from molpharm.aspetjournals.org at ASPET Journals on March 20, 2024

Molecular Pharmacology Fast Forward. Published on July 23, 2014 as DOI: 10.1124/mol.114.094128
This article has not been copyedited and formatted. The final version may differ from this version.

Figure 5

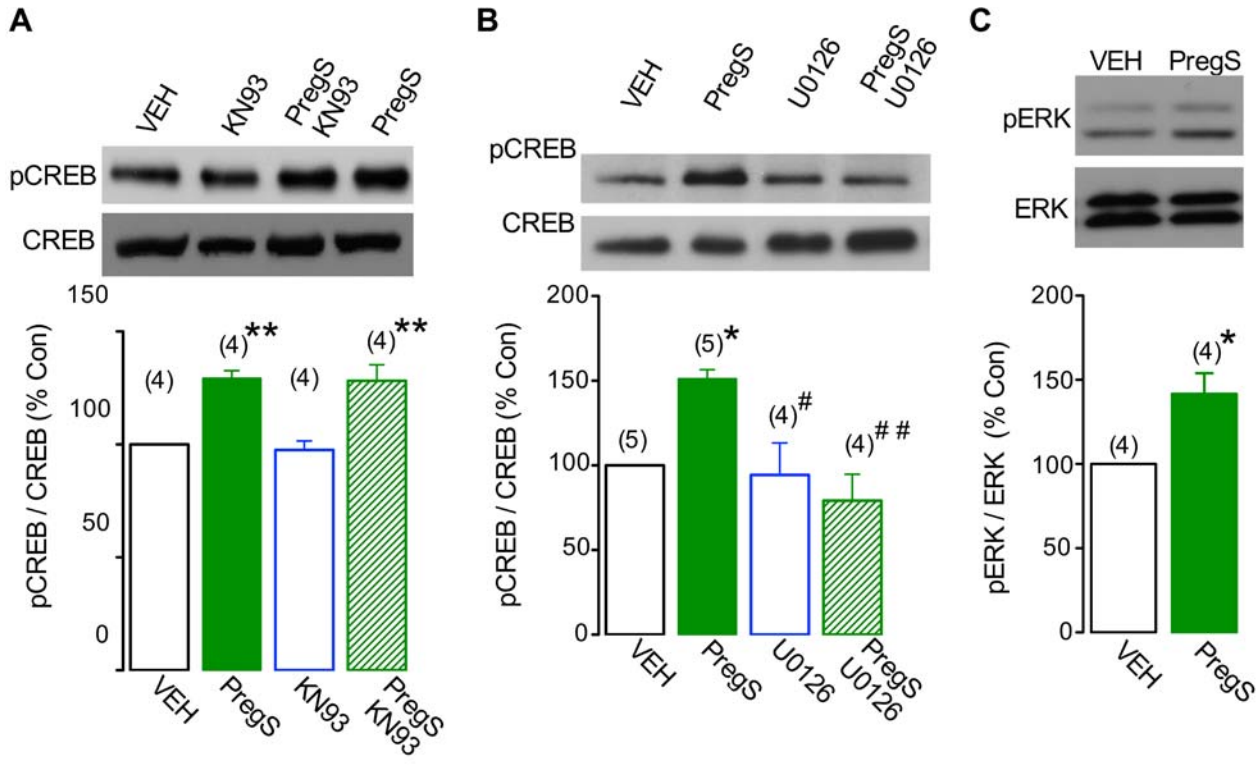

Downloaded from molpharm.aspetjournals.org at ASPET Journals on March 20, 2024

Molecular Pharmacology Fast Forward. Published on July 23, 2014 as DOI: 10.1124/mol.114.094128
This article has not been copyedited and formatted. The final version may differ from this version.

Figure 6

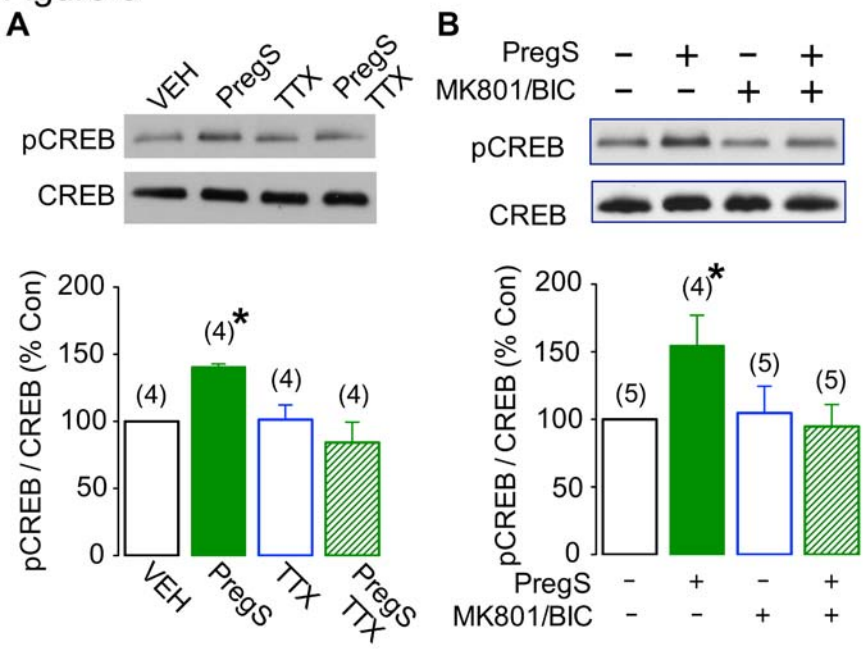

Downloaded from molpharm.aspetjournals.org at ASPET Journals on March 20, 2024

Molecular Pharmacology Fast Forward. Published on July 23, 2014 as DOI: 10.1124/mol.114.094128
This article has not been copyedited and formatted. The final version may differ from this version.

Figure 7

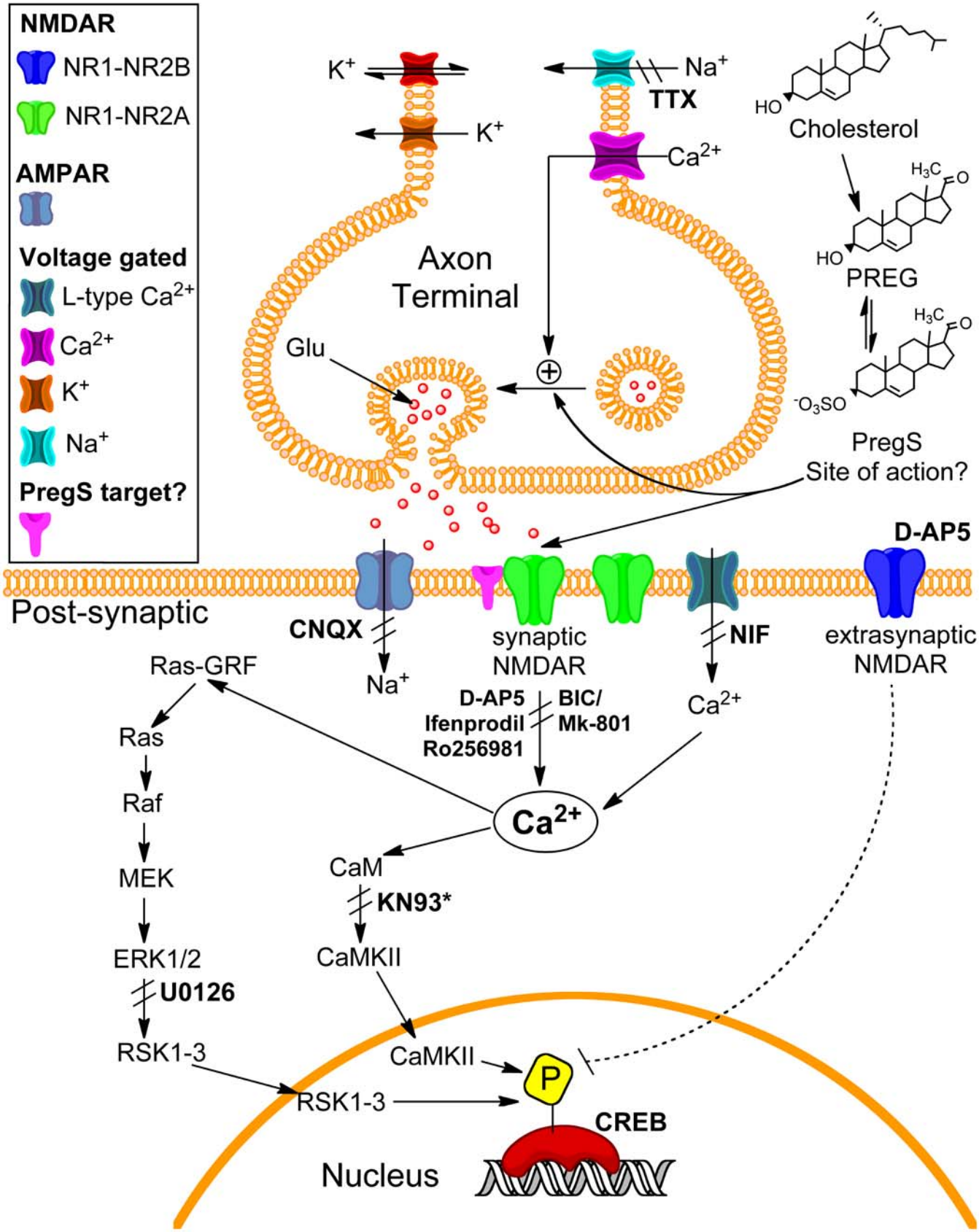

Downloaded from molpharm.aspetjournals.org at ASPET Journals on March 20, 2024